Adjusting the Structure, Band-gap, Optoelectronic Properties and Reactivity of Phenyl-2- Pyridyl Ketoxime via Functionalization with Chemical Groups: A Density Functional Theory Approach.

CHINYERE ANYAMA[1], AYI A. AYI[2]
[1, 2] *Department of Pure and Applied Chemistry, University of Calabar, Nigeria.*

Abstract- ***The structure of phenyl-2-pyridyl ketoxime (herein PPKO) with formula C12H10N2O extracted from literature and its CH3, OH, NH2 and NO2 modified forms were built with GUASS VIEW 6.0 and optimized at ground state with GAUSSIAN 09 using B3LYP (Beckes' 3-parameter exchange with Lee-Yang-Parr correlation energy) functional and 6-311+ G(d,p) basis set. Their structural, spectroscopic, optoelectronic and molecular properties were investigated at same molecular level. The HOMO - LUMO energy was used to calculate the quantum descriptors to gain insight into their band gap, reactivity and stability. From our result, we observed a narrowing of the energy gap of PPKO (0.184 eV) to 0.180 eV, 0.176 eV, 0.166 eV and 0.149 eV in CH3-PPKO, OH - PPKO, NH2-PPKO and NO2-PPKO respectively. The optical performance was calculated with Time dependent Self Consistent Field (TD - SCF) and Integral equation formalism polarizable continuum model (IEF - PCM) which is useful in studying vibrational circular dichroism and molecular properties in solution. From our result, the absorption wavelength of PPKO (283 nm) was extended to 284 nm, 307 nm and 356 nm in OH - PPKO, NH2-PPKO and NO2-PPKO respectively. This observed red shift in absorption wavelength is attributed to π-π* transitions. The simulated FT-IR and Raman spectroscopic information have been reported. The O-H stretch was observed at 3600 cm-1 , 3603 cm-1, 3605 cm-1, 3609 cm-1 and 3585 cm-1 for PPKO, CH3-PPKO, OH - PPKO, NH2-PPKO and NO2-PPKO respectively. The perturbation energy which gives insight into intramolecular and inter molecular interactions between donor and acceptor orbitals was calculated with respect to the second-order Fock matrix perturbation theory. NO2-PPKO showed the greatest perturbation energy (250.92 K/cal/mol) from transitions between π*C1-N6 and π*C4-C5 (donor and acceptor orbitals respectively).***

Indexed Terms- ***Bandgap, Stability, Perturbation energy, HOMO-LUMO, Absorption wavelength.***

I. INTRODUCTION

Phenyl-2-pyridyl ketoxime belongs to the family of oximes which are chemical compounds with the general molecular formula RR'C=NCH where R is an organic group, and R' hydrogen or an organic group. Phenyl -2- pyridyl ketoxime has the general formula RRC=NOH where R is a phenyl group and R' is a pyridyl group [1]. Phenyl-2-pyridyl ketoxime has a unique bonding capability and is able to form terminal, chelating and bridging bonds with most transition metals forming metal complexes with Cu^{2+}, Fe^{2+}, Mn^{2+}, Ni^{2+}, Ag^{2+}, Co^{2+} amongst others [2-11]. Chemists have also found interest in oximes as ligands because they are able to form mono-, di-, tri- and polynuclear copper complexes many of which are important magnetic and redox active materials [3]. Copper oximes possess biological active sites which enable them to bind covalently or non-covalently to Deoxyribonucleic acid (DNA) [5]. Since the discovery of MOFs by Omar Yaghi [12], there has been a lot of research going on in the area of metal-organic frameworks (MOFs) [13-18]. Scientists have found MOFs to be interesting materials because of their attractive properties which make them useful in many areas such as adsorption [19], catalysis [20], magnetism [21], storage [22], drug delivery [23], sensors [24] amongst others. MOFs are formed from inorganic metal cations and organic linkers (ligands) which act as antennas through which MOFs could absorb light. The properties of MOFs are highly dependent on the properties of the organic linkers

which makes the choice of ligand very important. A number of linkers have been reported in the synthesis of MOFs especially the carboxylates [25-28], pyridine [29-31], oximes [32-34] and many others. Improving or modifying the properties of MOFs could be achieved in various ways which includes mixing of ligands [35], grafting of active sites [36], impregnation of composite materials [37] and functionalization of ligands [38]. Millios *et al* reported the magnetic properties of mononuclear, trinuclear and octanuclear complexes of phenyl-2- pyridyl ketoxime [4], Li *et a*l reported the DNA-binding properties of four copper complexes based on a phenyl-2- pyridyl ketoxime ligand [39], Wong *et al* reported the reactivity of triosmium carbonyl clusters containing oxime ligands [10], Cheng *et al* reported a Luminescent Metal-Organic Framework with Lewis Basic pyridyl sites for the sensing of Metal ions [40]. Adjusting the properties of phenyl-2-pyridyl ketoxime in the synthesis of these metal complexes could be an efficient technique in adjusting the properties of the metal complexes. Moulin and co-workers reported the effect of ligand functionalization on the acid-base properties of flexible MOFs [41]. Hendon *et al* reported engineering the optical properties of the Ti-MIL125 MOF through ligand functionalization [42], Gregory et al reported tuning the adsorption properties of UiO-66 via Ligand Functionalization [43]. Zubair *et al* reported tuning the optoelectronic properties of indacenodithiophene based derivatives for efficient photovoltaic applications: A DFT approach.[44]. Abd-Elmageed and co-workers reported synthesis, DFT studies, fabrication, optical characterization of the (ZnCMC)TF polymer (organic/inorganic) as an optoelectronic device [45]. Afzai and Naqib reported a DFT based first - principles investigation of optoelectronic and structural properties of Bi2TeSe [46]. Babu and Vuai reported theoretical studies of optoelectronic and photovoltaic properties of D-A polymer monomers by density functional theory [47]. Tun-ability of MOFs with organic linkers is of obvious importance because it offers unlimited possibility to design functional or multifunctional organic linkers as well as unique chemical properties of organic groups. The purpose of this work is to investigate theoretically the possibility of adjusting the structure, band gap, optoelectronic and reactivity of PPKO directed towards the design of linker molecules which could form part of new complexes and MOF materials with enhanced properties. In this work, we present a detailed systematic investigation on the geometries, electronic structure, molecular properties, spectroscopic, optical absorption and reactivity of phenyl-2-pyridyl ketoxime (PPKO) functionalized with CH3, OH, NH2, and NO2.

II. COMPUTATIONAL DETAILS

The structure of phenyl-2-pyridyl ketoxime (herein PPKO) with formula $C_{12}H_{10}N_2O$ was extracted from literature, modified with CH3, OH, NH2 and NO2 and their structures were built with GAUSS VIEW 6.0 [48]. The entire calculations were performed using GAUSSIAN 09W [49] package and the geometry optimizations were performed at ground state using density functional theory (DFT) with Becke's three parameter exchange-functional combined with corrected correlation Lee, Yang and Parr functional (B3LYP) [50] functional with 6-311+G (d,p) basis set. The optical performance of the compounds in water, dimethylsulfoxide (DMSO) and chloroform was investigated with Time-dependent Self Consistent Field (TD - SCF) and Integral Equation Formalism Polarized Continuum Model (IEF - PCM) which is very useful in studying vibrational circular dichroism and molecular properties in solution.. Natural bond orbital (NBO) version 3.1 was used to study inter-molecular and intra - molecular charge transfer (ICT), conjugative interactions and electron density delocalization.

III. RESULTS AND DISCUSSION

3.1 Geometrical Parameters

The optimized structures, values of bond lengths, bond angles and dihedral angles calculated using Gaussian O9 and B3LYP 6-311 + G (d, p) are presented in Figure 1 and Tables 1, 2 and 3. From the result obtained, changes in all three parameters were observed which could be attributed to the presence of the groups in the PPKO framework. C1-C2 which was 1.395Å for PPKO was observed as 1.400 Å, 1.399 Å, 1.409 Å and 1.396 Å in CH3-PPKO, OH - PPKO, NH2-PPKO and NO2-PPKO respectively. C2-C3 was 1.390 Å, 1.395 Å, 1.391 Å, 1.397 Å and 1.388 Å for PPKO, CH3-PPKO, OH - PPKO, NH2-PPKO and NO2-PPKO respectively. C1-C2-C3 was observed as 117.9, 116.2, 118.1, 116.5 and 120.0 for PPKO, CH3-

PPKO, OH - PPKO, NH2-PPKO and NO2-PPKO respectively. C1-N6-C5 was 118.1, 118.8, 118.7, 118.3 and 119.0 respectively for PPKO, CH_3-PPKO, OH - PPKO, NH_2-PPKO and NO_2-PPKO. C2-C3-C4 was 118.8, 119.8, 118.3, 119.2 and 117.5 for PPKO, CH_3-PPKO, OH - PPKO, NH_2-PPKO and NO_2-PPKO respectively. There were also changes in the dihedral angles, C11-C10-C21-N22 was -109.1, -108.5, -108.4, -105.9 and -106.1 in PPKO, CH_3-PPKO, OH - PPKO, NH2-PPKO and NO2-PPKO respectively. C4-C5-C22-N23 was -155.8, -157.2, -157.9, -161.0 and -161.7 respectively for PPKO, CH_3-PPKO, OH - PPKO, NH2-PPKO and NO2-PPKO.

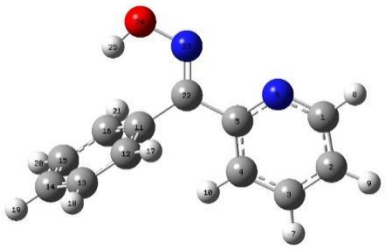

(a)

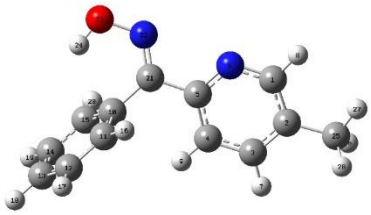

(b)

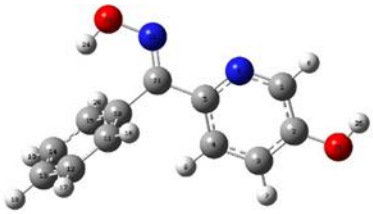

(c)

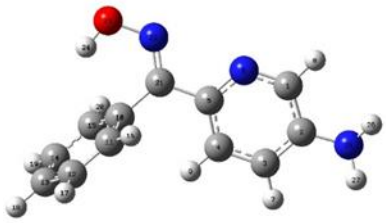

(d)

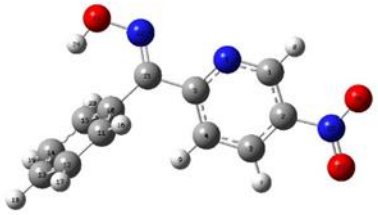

(e)

FIG 1. Optimized structures of PPKO (a), CH3-PPKO (b), OH - PPKO (c), NH2-PPKO (d) and NO2-PPKO (e).

Table 1: Selected Bond Length of Studied Compounds

BOND LENGTH	PPKO	CH3- PPKO
OH- lPPKO	NH2- PPKO	NO2- PPKO
C1-C2	1.395	1.400
1.399	1.409	1.396
C1-N6	1.331	1.330
1.325	1.322	1.326
C2-C3	1.390	1.395
1.391	1.397	1.388
C3-C4	1.390	1.389
1.388	1.388	1.386
C4-C5	1.402	1.402
1.403	1.401	1.405
C5-N6	1.341	1.339
1.340	1.343	1.344
C5-C21	1.491	1.490
1.489	1.487	1.478
C11-C12	1.401	1.392
1.392	1.392	1.392
C12-C13	1.392	1.394
1.395	1.304	1.394
C13-C14	1.394	1.393
1.393	1.393	1.393

C14-C15	1.393	1.394	
1.395	1.394	1.394	

Table 2: Selected Bond Angles of Studied Compounds.

BOND ANGLES	PPKO	CH3- PPKO	
OH- PPKO	NH2- PPKO	NO2- PPKO	
C1-C2-C3	117.9	116.2	
118.1	116.5	120.0	
C1-N6-C5	118.1	118.3	
118.8	119.0	118.7	
C2-C3-C4	118.8	119.8	
118.3	119.2	117.5	
C3-C4-C5	119.0	119.1	
119.7	119.8	119.2	
C4-C5-N6	122.1	121.6	
121.3	120.9	122.1	
N6-C5-C22	117.8	118.1	
118.2	118.3	117.8	
C10-C11-C12	120.4	120.4	
120.4	120.5	120.3	
C11-C12-C13	120.4	120.1	
121.1	120.2	120.1	
C12-C13-C14	119.8	119.8	
119.8	119.8	119.9	
C13-C14-C15	119.9	120.0	
120.1	120.1	120.0	

Table 3: Selected Dihedral Angles of Studied Compounds.

DIHEDRAL ANGLES	PPKO	CH3-PPKO	
OH-lPPKO	NH2-PPKO	NO2-PPKO	
C1-N6-C5-C22	-178.5	-178.5	
-178.3	-178.6	-178.9	
C3-C4-C5-C22	178.6	178.5	
178.4	178.6	179.0	
C4-C5-C22-N23	-155.8	-157.2	
-157.9	-161.0	-161.7	
C5-C22-C11-C16	-109.2	-108.5	
-108.4	-106.9	-106.0	
C5-C22-N23-O24	-178.5	-178.4	
-178.2	-178.3	-179.2	
C11-C22-C5-N6	-156.6	-158.0	
-158.9	-161.8	-162.5	
C12-C11-C22-N23	-109.2	-108.5	
-108.4	-106.8	-106.2	
C13-C12-C11-C22	179.6	179.7	
179.8	179.7	179.8	
C15-C16-C11-C22	-179.8	-179.9	
-179.9	-179.9	-179.9	

3.2 FRONTIER MOLECULAR ORBITALS (FMOs)

The highest occupied molecular orbital (HOMO) and the lowest unoccupied molecular orbital (LUMO) are referred to as frontier molecular orbitals (FMOs). The frontier orbital gap helps to characterize the chemical reactivity and the kinetic stability of the molecule [51]. A molecule with a small energy gap termed a soft molecule is generally associated with a high chemical reactivity and low kinetic stability [52]. The HOMO and LUMO structures and the orbitals for the studied molecules are shown in Figure 2. From our result the HOMO and LUMO of PPKO are the 52^{th} and 53^{th} orbital, the HOMO and LUMO of CH_3-PPKO, OH -PPKO and NH_2-PPKO are the 56^{th} and 57^{th} orbital, the HOMO and LUMO of NO_2-PPKO are the 63^{th} and 64^{th} orbital. The HOMO of PPKO is located over the C1-C2 and C4-C5-N6 bonds of the pyridyl ring and C=N and O atom of the ketoxime while the LUMO is delocalized over C2, C4, C5-C22 bond and N- atom of the pyridyl ring, the phenyl carbon atoms and the N-atom of the ketoxime. The HOMO of CH_3-PPKO is located over C1-C2 bond, C4-C5-N6 bond, CH3 group, C=N and O atom while LUMO is located over C2, C3, C5, N6, C5-C22 bond, N atom of ketoxime and the phenyl carbon atoms. The HOMO of OH -PPKO is located over C1-C2-C3 and C4-C5-N6 bond of the pyridyl ring, C=N, O atom of ketoxime and OH group while the LUMO is localized over C1-C2 and C5-C22 bonds, C3, N6, phenyl carbon atoms and N-atom of ketoxime. The HOMO of NH_2-PPKO is located over C1-C2-C3 and C4-C5-N6 bonds, NH_2 group, C=N and O atom of the ketoxime while the LUMO is located over C1-C2 and C5-C22, N- atom of the ketoxime and phenyl carbon atoms. The HOMO of NO_2-PPKO is located over C1-C2 and C4-C5-N6 bonds, C=N, O atom of ketoxime, C10-C15 and C13-C14 bonds of the phenyl ring while LUMO is located over the NO_2 group, C1, C2, C3, C5 and N6 of the pyridyl group and the N atom of the ketoxime. These (HOMO→LUMO) transitions suggest that electron density transfer was generally from the pyridyl ring to the phenyl ring. It also suggests that CH_3, OH and NH_2 are electron rich while NO_2 is electron deficient. From these HOMO-LIMO transitions, we also observe that

the ketoxime O atom is highly electron rich and so suggests that it could serve as coordination site for highly electron deficient metal cations.

3.3 Quantum Chemical Descriptors

The quantum chemical descriptors calculated with the famous Koopmans approximation [53] are presented in Table 4. On the basis of Koopmans approximation, the Ionization Potential (IP) and Electron Affinity (EA) are approximately equal to negative HOMO (-HOMO) and negative LUMO (-LUMO) respectively.

$IP = -E_{HOMO}$ (1)

$EA = -E_{LUMO}$ (2)

Using equations (3) – (7) the global reactivity descriptors can be calculated as is reported in literature [16, 25].

The hardness ofthe molecule is $\eta=(IP-EA)/2$. (3)

The chemical potential of the molecule is $\mu=-(IP+EA)/2$. (4)

The softness(σ) of the molecule= $1/2\eta$. (5)

The electronegativity of the molecule is $\chi = (IP+EA)/2$. (6)

The electrophilicity index of the molecule is $\omega = \mu/2\eta 2$. (7)

A molecule with lower value of ionization potential is a better electron donor while a molecule with higher value of electron affinity is a better electron acceptor. A molecule with higher softness and lower hardness value is more reactive, less stable and more polarizable. From our result, NH2-PPKO with the lowest ionization potential value (0.217 eV) is the best donor while NO_2-PPKO with the highest electron affinity value of 0.119 eV is the best acceptor. We can also deduce from our result that the energy gap of PPKO (0.184 eV) was narrowed down to 0.180 eV, 0.176 eV, 0.166 eV and 0.149 eV in CH_3-PPKO, OH - PPKO, NH_2-PPKO and NO_2-PPKO respectively which is in good agreement with the softness values of 5.425, 5.528, 5.761, 6.023 and 6.673 for PPKO, CH_3-PPKO, OH - PPKO, NH_2-PPKO and NO_2-PPKO respectively. The lower the energy gap, the more reactive a molecule and so NO_2-PPKO with the lowest energy gap (0.149 eV) is the most reactive with the highest softness value of 6.673 which suggests it is less stable and most polarizable. These results show that functionalization of PPKO with these chemical groups narrowed the band gap of PPKO thereby increasing its reactivity. These properties which can be transferred from the linkers (PPKO, CH_3-PPKO, OH - PPKO, NH_2-PPKO, NO_2-PPKO) to the metal complexes and MOFs during syntheses could enhance or modify their catalytic, semi-conductor, reactivity and optoelectronic properties.

Table 4: Quantum Chemical Descriptors of Studied Compounds

	PPKO	CH_3-PPKO	OH - PPKO	NH_2-PPKO	NO_2-PPKO
E_{HOMO} (eV)	- 0.2467	- 0.2402	- 0.2341	- 0.2170	- 0.2697
E_{LUMO} (eV)	-0.0624	- 0.0593	- 0.0578	-0.0510	- 0.1199
ΔE_{gap} (eV)	0.1843	0.1808	0.1763	0.1660	0.1498
IP (eV)	0.2467	0.2402	0.2341	0.2170	0.2697
EA (eV)	0.0624	0.0593	0.0578	0.0510	0.1199
μ (eV)	-0.1545	-0.1498	-0.1460	-0.1346	-0.1948
χ (eV)	0.1545	0.1240	0.1460	0.1346	0.1948
η (eV)	0.0921	0.0904	0.0881	0.0830	0.0749
σ (eV)	5.4256	5.5282	5.6711	6.0233	6.6737
ω (ev)	0.1296	0.1214	0.1208	0.1092	0.2534

3.4 Vibrational Analysis

Vibrational analysis enables us to determine the vibrational modes associated with relevant and specific molecular structures of the calculated molecules studied. The maximum number of potentially active observable fundamentals of a non-linear molecule which contains N atoms is equal to (3N-6) normal modes of vibration [54]. Hence, PPKO molecule has 25 atoms with 69 vibrations, CH_3--PPKO has 28 atoms with 69 vibrations, OH - PPKO has 26 atoms with 72 vibrations, NH_2-PPKO and NO_2-PPKO have 27 atoms each with 75 vibrations. The IR

spectra of the studied molecules are presented in Figure 2 while the frequencies, intensities and vibrational assignments are presented in S9. C-C vibration was observed at 1288 cm^{-1}, 1284 cm^{-1}, 1281 cm^{-1}, 1288 cm^{-1} and 1302 cm^{-1} for PPKO, CH_3-PPKO, OH - PKO, NH_2-PPKO and NO_2-PPKO respectively. C=C stretching vibrations was observed at 1596 cm^{-1}, 1588 cm^{-1} and 1508 cm^{-1}, 1596 cm^{-1} and 1625 cm^{-1} for PPKO, CH_3-PPKO, OH - PKO, NH_2-PPKO and NO_2-PPKO respectively. C=N vibrations was observed at 1619 cm^{-1}, 1642 cm^{-1}, 1616 cm^{-1} and 1595 cm^{-1} for CH_3-PPKO, OH - PKO, NH_2-PPKO and NO_2-PPKO respectively. C-H stretching vibrations for PPKO was observed at 3145 cm^{-1} while for CH_3-PPKO, OH - PPKO, NH_2-PPKO and NO_2-PPKO it was observed at 3130 cm^{-1}, 3106 cm^{-1} 3115 cm^{-1} and 3194 cm^{-1} respectively while the O-H stretch is observed at 3600 cm^{-1}, 3603 cm^{-1}, 3605 cm^{-1}, 3609 cm^{-1} and 3585 cm^{-1} for PPKO, CH_3-PPKO, OH - PKO, NH_2-PPKO and NO_2-PPKO respectively. NH_2 symmetric, asymmetric and bending vibrations were observed at 3573 cm^{-1}, 3673 cm^{-1} and 1662 cm^{-1}respectively for NH_2-PPKO while the CH_3 vibrations for CH_3-PPKO was observed at 3024 cm^{-1}.

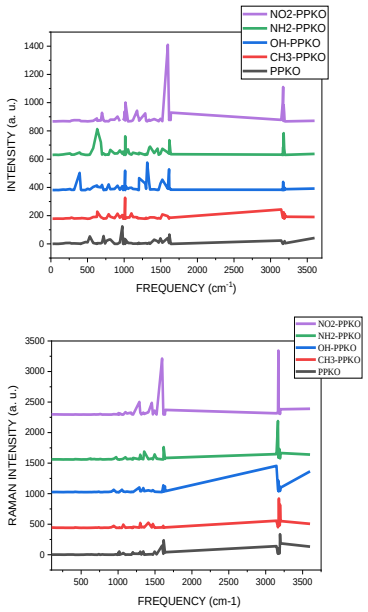

Figure 2. Simulated IR and Raman spectra of studied compounds.

3.5 UV - vis Spectroscopic Analysis

The electronic activities of the molecules have been estimated by TD-SCF/IEF -PCM/B3LYP 6-311 + G (d,p). The UV-visible spectra of the molecules in water, dimethyl sulfoxide and chloroform are presented in Figure 3 while the wave lengths (λ_{max}), excitation energy (E) and oscillator strengths are presented in S7, S8 and S9. From our result, the spectra of the studied compounds show one peak each at wavelengths 283 nm for PPKO and CH_3-PPKO, 284 nm, 307 nm and 356 nm (λ_{max}) for OH - PPKO, NH_2-PPKO and NO_2-PPKO in water, In DMSO 283 nm was observed for PPKO and CH_3-PPKO, 285 nm, 308 nm and 356 nm for OH-PPKO, NH_2-PPKO and NO_2-PPKO while 286 nm for PPKO and CH_3-PPKO, 285 nm, 307 nm and 356 nm were observed for OH - PPKO, NH_2-PPKO and NO_2-PPKO respectively in chloroform. These transitions corresponding to $\pi \rightarrow \pi^*$ transition is governed by HOMO →LUMO excitation. From our result, we observe that absorption wavelength of PPKO was extended remarkably from 283 nm to 307 nm and 356 nm in NH_2-PPKO and NO_2-PPKO respectively. This red shift observed shows that the optical property of PPKO was enhanced by functionalizing it with the chemical groups. These extensions increase as band gap decrease thus suggesting that the optoelectronic property of PPKO was adjusted.

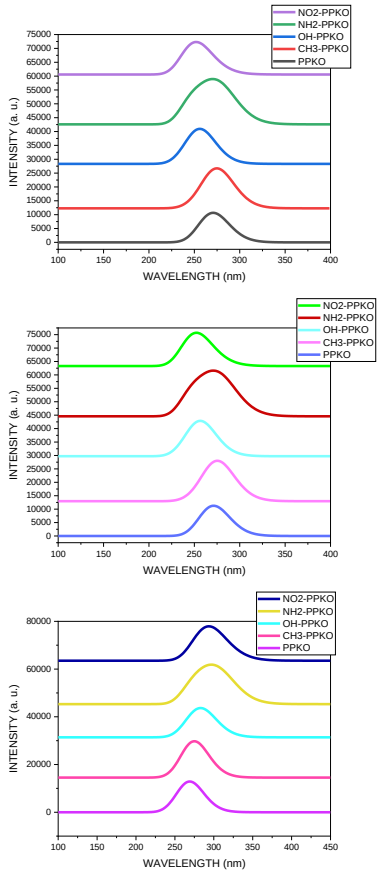

(a) (b)

(c)

Figure 3. Simulated UV - Vis spectra of studied compounds in water (a), DMSO (b), and chloroform (c) calculated with B3LYP/6-311 +G (d,p) basis sets.

3.6 Natural Bonding Orbital (NBO) Analysis.

Natural bond orbital (NBO) analysis provides an effective technique for studying intra- and inter molecular bonding interactions between bonds and also presents a suitable basis for investigating charge transfer or conjugative interactions in molecules [55]. The greater the perturbation energy value, the stronger the interaction between the electron donors and the more the conjugation of the system [56-57]. The second-order perturbation energy values of PPKO, CH_3-PPKO, OH - PKO, NH_2-PPKO and NO_2-PPKO were calculated with respect to the second-order Fock matrix perturbation theory using DFT/B3LYP/6-311+G (d, p) functional. The most interacting NBOs are presented in S1, S2, S3, and S4 for PPKO, CH_3-PPKO, OH - PKO, NH_2-PPKO and NO_2-PPKO respectively. From our result, molecular interactions in the studied molecules is observed by a π-π*, π*-π* transition between C–C orbitals and π-LP, π-LP*, LP-π*, LP-LP*, LP*-π* transition between C-C, O-C, N-C and O-N orbitals. Hyper intra-molecular conjugative interactions in the molecules is formed by the orbital overlap between π*C1-N6 and π*C4-C5 for PPKO, LP(1)C2 and π*C1-N6 for CH_3-PPKO, π*C1-N6 and π*C4-C5 for OH - PPKO, LP(1)C5 and π*C1-C6 for NH_2-PPKO, π*C5-N6 and π*C3-C4 for NO_2-PPKO producing stabilization energies 250.92 K/cal/mol, 89.04 K/cal/mol, 170.08 K/cal/mol, 75.72K/cal/mol and 228 K/cal/mol for PPKO, CH_3-PPKO, OH - PKO, NH_2-PPKO and NO_2-PPKO respectively. The greater the perturbation energy, the more stable and conjugated a system. The more the conjugation, the less the reactivity of a molecule. From our result, PPKO has highest perturbation energy which suggests that it is more stable and less reactive which agrees with the fact that it had the highest energy (ΔEgap) value.

3.7 Charge Analysis

Mulliken charges is one of the population analyses which emanates from the Mulliken population analysis (MPA) and is required for the evaluation of partial atomic charges from calculations using the methods of computational chemistry on the basis of linear combination of atomic orbitals [58]. MPA analysis is highly effective in determining the size, structure and electronic distribution of the HOMO - LUMO orbitals, which is key in predicting the concentration of electrons in the studied molecules. A plot of Mulliken charge distribution with number of atoms for the molecules is presented in Figure 4. From our result, the most electropositive atom (most susceptible to nucleophillic attack) in PPKO is C11 (1.588 a. u.) while the most electronegative atom (most susceptible to electrophillic attack is C22 (-0.959 a. u.). The most electropositive atom (most susceptible to nucleophillic attack) in CH_3-PPKO is C10 (1.261a. u.) while the most electronegative atom (most susceptible to electrophillic attack) is C5 (-0.870 a. u.). The most electropositive atom (most susceptible to nucleophillic attack) in OH-PPKO is C10 (0.929 a. u.) while the most electronegative atom (most susceptible to electrophillic attack is C5 (-0.780 a. u.). The most electropositive atom (most susceptible to nucleophillic attack) in NH_2-PPKO is C10 (1.160 a. u.) while the most electronegative atom (most susceptible to electrophillic attack) is C5 (-0.760 a. u.). The most

electropositive atom (most susceptible to nucleophillic attack) in NO_2-PPKO is C10 (1.400 a. u.) and the most electronegative atom (most susceptible to electrophillic attack) is C5 (-0.602 a. u.). Our result suggests more interaction within the pyridyl ring (C5 and C10) in the functionalized PPKO molecules which is attributed to the presence of the chemical groups. Also from our result, C2 (point of attachment of chemical groups) atomic charge was positive for PPKO and CH_3-PPKO (0.062 a. u. and 0.784 a. u. respectively) while for OH - PPKO, NH_2-PPKO and NO_2-PPKO it was negative (-0.128 a. u., -0.025 a. u. and -0.068 a. u. respectively). This also suggests changes in electron density caused by the presence of the chemical groups on the C2 atom.

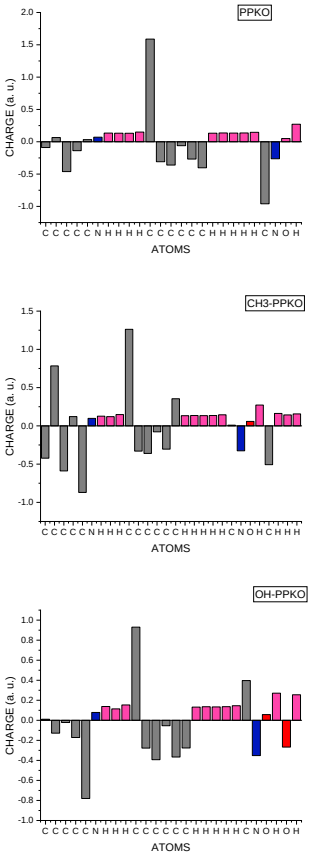

(a) (b) (c)

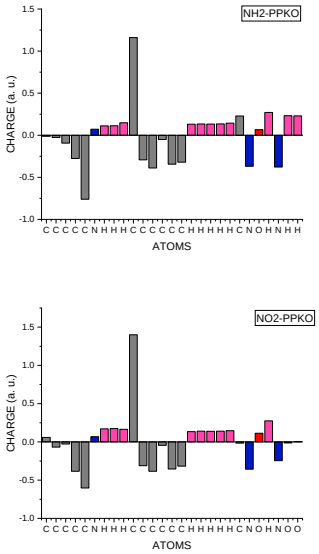

(d) (e)

Figure 4. A plot of Mulliken Atomic Charge Distributions with Number of Atoms for PPKO (a), CH_3-PPKO (b), OH - PPKO (c) and NH_2-BTC (d) and NO_2-PPKOrespectively.

CONCLUSION

This research was carried out to adjust the structure, band gap, optoelectronic properties and reactivity of phenyl 2- pyridyl ketoxime. From the result obtained changes in all three geometrical parameters were observed which can be attributed to the presence of the groups in the PPKO framework. For instance, C1-C2 which was 1.395Å for PPKO was observed as 1.400 Å, 1.399 Å, 1.409 Å and 1.396 Å in CH_3-PPKO, OH - PPKO, NH_2-PPKO and NO_2-PPKO respectively. From our result, the energy gap of PPKO (0.184 eV) was narrowed down to 0.180 eV, 0.176 eV, 0.166 eV and 0.149 eV in CH3-PPKO, OH - PPKO, NH_2-PPKO and NO2-PPKO respectively which is in good agreement with their softness values of 5.425, 5.528, 5.761, 6.023 and 6.673 for PPKO, CH_3-PPKO, OH - PPKO, NH_2-PPKO and NO_2-PPKO respectively. The lower the energy gap, the more reactive a molecule and so NO_2-PPKO with the lowest energy gap (0.149 eV) is the most reactive with the highest softness value of 6.673. This result shows that functionalization of PPKO with these chemical groups narrowed the band gap of PPKO thereby increasing its reactivity. From our result, we observed that absorption wavelength of PPKO was extended remarkably from 283 nm to 307

nm and 356 nm in NH_2-PPKO and NO_2-PPKO respectively. This red shift observed suggest that the optical property of PPKO was enhanced by functionalizing it with the chemical groups. These extensions increase as band gap decrease thus also suggesting that the optoelectronic property of PPKO was adjusted. These properties which could be transferred from the linkers (PPKO, CH_3-PPKO, OH - PPKO, NH_2-PPKO, NO_2-PPKO) to the metal complexes and MOFs during syntheses could enhance or modify their band gap, reactivity, optoelectronic, catalytic and semi-conductor properties thereby giving a wide array of unique hybrid materials that could be useful in relevant areas.

REFERENCES

[1] Milios, C. J., Stamatatos, T. C., and Perlepes, S. P. (2006). The coordination chemistry of pyridyl oximes. Polyhedron. 25, 134-194. doi: 10.1016/j.ica.2007.06.031

[2] Mohan, M., and Paramhans, B. D. (1981). Transition Metal Chemistry of Oxime-Containing Ligands, Part XIV. Iron (II) Complexes of syn-Phenyl-2- pyridylketoxime and syn-Methy 1-2-pyridylketoxime. Croatia Chemical Acta.54, 173-182.

[3] Szczęsny, R., Szłyk, E., Kozakiewicz, A., Dobrzańska, L. (2017). Thermal and structural characterization of copper (II) complexes with phenyl-2-pyridylketoxime (HPPK). Journal of Thermal Analysis and Calorimetry. 128, 1591-1599 DOI https://doi.org/10.1007/s10973-016-5956-y

[4] Milios, C. J., Stamatatos, T. C., Kyritsis, P., Terzis, A., Raptopoulou, C. P.,Vicente, et al (2004). Phenyl 2-Pyridyl Ketone and Its Oxime in Manganese Carboxylate Chemistry: Synthesis, Characterisation, X-ray Studies, and Magnetic Properties of Mononuclear, Trinuclear and Octanuclear Complexes. European Journal of Inorganic Chemistry 14,2885-901 DOI: 10.1002/ejic.200400035

[5] Li, R., Lu, J., Li, D., Cheng, S., Dou, J. (2014). Syntheses, structures, in vitro cytotoxicities, and DNA-binding properties of four copper complexes based on a phenyl 2-pyridyl ketoxime ligand. Transition Metal Chemistry, 39, 507-517. DOI:10.1007/s11243-014-9826-9

[6] Hołyńska, M. (2015). The structural variety and magnetic properties of oxime-bridgedcopper (II) complexes. Journal of Molecular Structure.1098,175-180 https://doi.org/10.1016/j.molstruc.2015.06.014

[7] Carcelli, M., Cozzini, P., Marroni, R., Pelagatti, P., Pelizzi, C., and Sgarabotto, P. (1999). Unusual coordination mode of a 2-pyridyl ketone oxime ligand in bis (4-butyl phenyl 2-pyridyl ketone oximate) palladium (II). Inorganica Chimicta Acta. 285, 138-141 https://doi.org/10.1016/S0020-1693(98)00299-0

[8] Hołyńska, M. (2013). Iridium (III) products isolated in a reaction of IrCl3 with phenyl 2-pyridyl ketoxime. Z. Kristallogr – Cryst. Mater. 228, 72-76 DOI:10.1524/zkri.2012.1576

[9] Yin, J. Z., and Liu, G. X. (2009). Dichloridobis (phenyl 2-pyridyl ketone oxime) nickel (II) acetone solvate. Acta. Crystallographica E. 65, m155-m155 doi: 10.1107/S1600536808043961

[10] Wong, J. S. Y., and Wong, W. T. (2002).Synthesis, structural characterization, and reactivity of triosmium carbonyl clusters containing oxime ligands. New Journal of Chemistry. 26, 94-104 DOI:10.1039/b107628k

[11] Chen, W. Q., Chen, Y. M., Lei, T., Liu, W., and Li, Y. (2012). V-shaped Fe3III and linear FeII/FeIII/FeII complexes supported by phenyl-pyridine-2-yl-methanone oxime ligand: Solvothermal syntheses, structures, and magnetic property. Inorganic ChemicalCommunication19,49https://doi.org/10.1016/j.inoche.2012.01.015

[12] Li, H., Eddaoudi, M., O'Keeffe, M. & Yaghi, O. M. (1999), Design and synthesis of a exceptionally stable and highly porous metal-organic framework. *Nature*, 402, 276-279 https://doi.org/10.1038/46248

[13] Allendorf, M. D., Houk, R. J. T., Andruszkiewicz,L., Talin, A. A., Pikarsky, J., et al (2008). Stress-induced chemical detection using flexible metal− organic frameworks. *Journal of American Chemical Society*, 130, 14404-14405 https://doi.org/10.1021/ja805235k

[14] Bauer, C.A., Timofeeva,T. V., Settersten, T. B., Patterson, B. D., Liu, V. H et al (2007). Influence of connectivity and porosity on ligand-based

luminescence in zinc metal−organic frameworks. *Journal of American Chemical Society*, 29, 7136-7144 https://doi.org/10.1021/ja0700395

[15] Chandler, B. D., Cramb, D.T., Shimizu, G.K.H. (2006). Microporous metal−organic frameworks formed in a stepwise manner from luminescent building blocks. *Journal of American Chemical Society*, 128, 10403-10412.ttps://doi.org/10.1021/ja060666e

[16] Chinyere, A. A., Providence B. A., Bassey E. I., Idongesit J. M., Ayi A. A. (2019) Metal-Organic Frameworks as Precursor for Metal Oxide Nanostructures Part I: MOF-Derived Copper Oxide Embedded in Carbon Matrix. Advanced Journal of Chemistry Section A, 2(3), 234-244 doi: 10.33945/SAMI/AJCA.2019.2.234244

[17] Cui, Y., Xu, H., Yue, Y., Guo, Z., Yu, J., et al (2012). A luminescent mixed-lanthanide metal–organic framework thermometer. *Journal of American Chemical Society*, 134, 3979 - 3982.https://doi.org/10.1021/ja2108036

[18] Dey, C., Kundu, T., Biswal, B. P., Mallick. A., Banerjee, R. (2014). Crystalline metal-organic frameworks (MOFs): synthesis, structure and function. Acta Crystallographica, B 70, 3–10 DOI:10.1107/S2052520613029557

[19] Li, J. R., Kuppler, R. J., Zhou, H.C. (2009). Selective gas adsorption and separation in metal-organic frameworks. *Chemical Society Review*, 38, 1477-1504.DOI https://doi.org/10.1039/B802426J

[20] Xiang, W., Zhang, Y., Lin, H., Liu, C. J. (2017). Nanoparticle/Metal-Organic Framework Composites for Catalytic Applications: Current Status and Perspective. *Molecules*, 22: 2103.https://doi.org/10.3390/molecules2212210 3

[21] Kurmoo, M. (2009). Magnetic metal–organic frameworks *Chemical Society Review*, 38:1353-1379.DOI https://doi.org/10.1039/B804757J

[22] Konstas, K., Osl, T., Yang, Y., Batten, M., Burke, N., et al (2012). Methane storage in metal organic frameworks. Journal of Material Chemistry, 22, 16698-16708.Dhttps://doi.org/10.1039/C2JM32719H

[23] Keke S., Ling L., XiaoLan Y., Li L., Qingtao M., et al (2017). Functionalization of mixed ligand metal-organic frameworks as the transport vehicles for drugs. *Journal of Colloid Interface Science*, 486,128-135.DOI:10.1016/j.jcis.2016.09.068

[24] Lu, Z. Z., Zhang, R., Li, Y. Z., Guo, Z. J., Zheng, H. G. (2011). Solvatochromic behaviour of a nanotubular metal-organic framework for sensing small molecules. *Journal of American Chemical Society*, 133, 4172-4174. https://doi.org/10.1021/ja109437d

[25] Anyama C.A., Ita B.I., Ayi A.A., Loius H, Okon E.D.D., et al (2021). Experimental and Density Funtional Theory studies on a Zinc (II) Coordination Polymer Constructed with 1,3,5-Benzenetricarboxylic Acid and Derived Nanocompsites from Activated Carbon. ACS Omega, 6, 28967-28982 DOI:10.1021/acsomega.1c04037

[26] Esther E., Louis, H.M., Chinyere A. A., Joseph O. O., Patrick M. U., et al (2020), Experimental and density functional theory studies on the adsorption behavior of selected gas molecules on Mg(II) coordination polymer constructed with 1,3,5- benzenetricarboxylates Journal of Molecular Structure, 1220(2020)128641https://doi.org/10.1016/j.molstruc.2020.128641.

[27] Nurettin S., Sahin D., Mustafa Y. (2017). Preparation and Characterization of Bi-metallic and Tri-metallic Metal Organic Frameworks Based on Trimesic Acid and Co(II), Ni(II), and Cu(II) Ions *Journal of Electronic Materials* 46, 790–801.https://doi.org/10.1007/s11664-016-4969-4

[28] Lin, X., Telepeni, I., Blake, A. J., Dailly, A., Brown, C. M., et al (2009). High capacity hydrogen adsorption in Cu(II) tetracarboxylate framework materials: the role of pore size, ligand functionalization, and exposed metal sites. *Journal of American Chemical Society*, 131, 2159 -2171https://doi.org/10.1021/ja806624j

[29] Ohi, H., Tachi, Y., Itoh, S.(2004). Supramolecular and Coordination Polymer Complexes Supported by a Tripodal Tripyridine Ligand Containing a 1,3,5-Triethylbenzene Spacer, *Inorganic Chemistry*, 43, 4561-45634. DOI: 10.1021/ic049468j

[30] An, J., Geib, S. J., Rosi, N. L. (2010). High and Selective CO_2 Uptake in a Cobalt Adeninate Metal-Organic Framework Exhibiting Pyridine

and Amino-Decorated Pores. *Journal of American Chemical* Society, 132, 38-39. DOI: 10.1021/ja909169x

[31] Carson, C. G., Brown, A. J., Sholl, D. S., Nair, S. (2011). Sonochemical Synthesis and Characterization of Submicrometer Crystals of the Metal-Organic Framework Cu[(hfipbb)(H2hfipbb) 0.5] *Crystal Growth and Design*, 11, 4505–4510.DOI:10.1021/cg200728b

[32] Constantinos, G. E., Loannis, M., Sayak, D. G., Anastasios, T., Vassilios, N., et al (2019). Synthesis and characterisation of new Ni_2Mn, Ni_2Mn_2 and Mn_8 clusters by the use of 2-pyridyl oximes Polyhedron 171, 330-337 DOI:10.1016/j.poly.2019.07.024

[33] Javier, M., Iolinda, A., Anna, B., Alessandra, C., Mauro, G. (2008). Tetranuclear zinc complexes of ligands containing the 2-pyridyl oxime chelating site Inorganica Chimica Acta 361, 2677-2682 https://doi.org/10.1021/ic00113a005

[34] Olajuyigbe A. A., Khalil A. A., George C, (2017). Mn3 Single-Molecule Magnets and Mn6/Mn9 Clusters from the Use of Methyl 2-Pyridyl Ketone Oxime in Manganese Phosphinate and Phosphonate Chemistry. Inorganic Chemistry 56, 11352–11364 American Chemical Society. DOI: 10.1021/acs.inorgchem.7b01793

[35] Keke S., Ling L., XiaoLan Y., Li L., Qingtao M., et al (2017). Functionalization of mixed ligand metal-organic frameworks as the transport vehicles for drugs. *Journal of Colloid Interface Science* 486,128-135. DOI: 10.1016/j.jcis.2016.09.068

[36] Zhang, W., Chen, Z., Al-Naji, M., Guo, P., Cwik, S. et al. (2016). Simultaneous introduction of various palladium active sites into MOF via one-pot synthesis: Pd@[Cu_3xPdx(BTC)2]n. *Dalton Transactions*, 45, 14883–14887. DOI https://doi.org/10.1039/C6DT02893D

[37] Ke, F., Wang, L., Zhu, J. (2015). Facile fabrication of CdS-metal-organic framework nano composites with enhanced visible-light photo catalytic activity for organic transformation. *Nano Research*, 8, 1834–1846. https://doi.org/10.1007/s12274-014-0690-x

[38] Gemechis, D. D., Ravindr, P., Chansi, G., Lalit, B (2019).Tailoring of the electronic property of Zn-BTC metal–organic framework *via* ligand functionalization: an *ab initio* investigation† *Royal Society of Chemistry Advances* , 25, 13959 – 14579.DOI https://doi.org/10.1039/C9RA00687G

[39] Li, J. R., Kuppler, R. J., Zhou, H.C. (2009). Selective gas adsorption and separation in metal-organic frameworks. *Chemical Society Review*, 38, 1477-1504.DOI https://doi.org/10.1039/B802426J

[40] Chen, B. L., Wang, L. B., Xiao, Y. Q., Fronczek, F. R., Xue, M., et al (2009). A Luminescent Metal-Organic Framework with Lewis Basic pyridyl sites for the sensing of Metal ions, *Angewandte Chemie International Edition*, 48, 500-503.DOI: 10.1002/anie.200805101

[41] Beatrice, M., Fabrice S., Sandrine, B., Philip, L. L., Thomas D., et al (2014). Effect of the ligand functionalization on the acid–base properties of flexible MOFs. *Microporous and Mesoporous Materials* 195,197–204.DOI:10.1016/j.micromeso.2014.04.025

[42] Christopher H., Hendon, D., Tiana, M., Fontecave, C., Sanchez, L et al (2013). Engineering the optical response of the titanium-MIL-125 metal-organic framework through ligand functionalization. *Materials Science Journal of the American Chemical Society*, 135, 10942-10945 https://doi.org/10.1021/ja405350u

[43] Gregory, E. C., Min, K., Seth, M. C., Krista S. W (2012). Tuning the Adsorption Properties of UiO-66 via Ligand Functionalization. *Langmuir* 28, 15606–15613.· DOI: 10.1021/la3035352

[44] Zubair, I., Ahmad, R., Sahar, K., Akram, j.,El-Badry, Y. A., et al (2022). Tuning The Optoelectronc Properties of indacenodithiophene Based Derivatives for Efficient Photovoltaic Applications: A DFT approach. *Chemical Physics Letters*, 793, 139459.https://doi.org/10.1016/j.cplett.2022.139459

[45] Abd-Elmageed, A. A. I., Ibrahim, S. M., Al-Hossainy A. F. (2020). Synthesis, DFT Studies, Fabrication, and Optical Characterization of the (Zn CMC)^{TF} Polymer (organic/inorganic) as an Optoelectronic Device. *New Journal of Chemistry*, 44, 8621-8637 DOIhttps://doi.org/10.1039/D0NJ01719A

[46] Afzai, M. A., Naqib S. H. (2021). A DFT Based First - Principles Investigation of Optoelectronic and Structural Properties of Bi2Te2Se. Physica Scripta, 96, 045810.Afzai, M. A., Naqib S. H. (2021). A DFT Based First - Principles Investigation of Optoelectronic and Structural Properties of Bi2Te2Se. Physica Scripta, 96, 045810.DOI:10.1088/1402-4896/abe2d2

[47] Babu, N. S., Vuia A. H. (2021), Theoritical Studies of Optoelectronic and Photovoltaic Properties of D-A Polymer Monomers by Density functional Theory (DFT). *Designed Monomers and Polymers*, 24, 226-239· DOI: 10.1080/15685551.2021.1956209

[48] Dennington, R., Keith, T. A., Millam, J. M. (2016). Gauss View 6.0 16, Semichem Inc., Shawnee Mission, KS, USA.

[49] M.J. Frisch, G.W. Trucks, H.B. Schlegel, G.E. Scuseria, M.A. Robb, J.R. et al (2009) Gaussian 09, Revision C. 02, Gaussian, Inc., Wallingford CT

[50] Parr, R. G &Yang. W. (1984). Density functional approach to the frontier-electron theory of chemical reactivity. *Journal of American Chemical Society* 106, 4049-4050.https://doi.org/10.1021/ja00326a036

[51] Pearson, R. G. (1993). The principle of maximum hardness, Accounts of Chemical Research, 26, 250–255https://doi.org/10.1021/ar00029a004

[52] Koopmans, T. (1993). About the assignment of wave functions and eigenvalues to the individual electrons of an atom. *Physicia Polonica* (1-6) 104-113. https://doi.org/10.1016/S0031-8914(34)90011-2

[53] Roeges, N.P.G., A Guide to the Complete Interpretation of Infrared Spectra of Organic Structures, Wiley, New York, 1994.

[54] Chen, J., Zhao, H., Farajtabar, A., Zhu, P., Jouyban, A., et al (2022). Equilibriumsolubility of amrinone in aqueous co-solvent solutions reconsidered: quanti-tative molecular surface, inter/intra-molecular interactions and solvation ther-modynamics analysis, Journal of Molecular Liquids 355 (2022) 118995DOI:10.1016/j.molliq.2022.118995

[55] Kramer, C. A. C., da Silva, A. R. L., de Lima-Neto, P., L.S. de Carvalho, L. S. (2022) Computational approach in lignin structural models: influence of non-covalent intramolecular interactions on βO4 bond properties, Journal of Molecular Structure, 1251 (2022)131938.DOI:10.1016/j.molstruc.2021.131938

[56] Mulliken, R. S. (1995). Electronic population analysis on LCAO-MO molecular wave functions. International Journal of Chemical Physics 23, 1833–1840.http://dx.doi.org/10.1063/1.1740588